Mon. Not. R. astr. Soc. (1974) **166,** 305–327.

OBSERVATIONS OF CYGNUS A WITH THE 5-KM RADIO TELESCOPE

P. J. Hargrave and M. Ryle

(Received 1973 August 20)

SUMMARY

Maps of the distribution of radio brightness and polarization in Cygnus A at 5 GHz have been made with an angular resolution of $2''{\cdot}0 \times 3''{\cdot}1$ arc. These show details of the structure of the compact features in the parts of the source most distant from the optical galaxy, as well as the structure and particularly the strong polarization in parts of the extensive tails. Some limited observations at 15 GHz with a resolution of $0''{\cdot}4$ arc have been used to define more closely the shape of the compact components. A weak central source $< 1{\cdot}5$ kpc in diameter has been found which lies between the two optical ' nuclei ' in photographs of the central region of the galaxy.

On the assumption of equipartition between relativistic electrons and magnetic field, and from a study of the spectral distribution, it is concluded that there must be a continuous replenishment of energetic electrons within each of the two main compact components of the source, representing an energy supply of $\sim 10^{45}$ erg s^{-1}. These electrons must diffuse out into the extensive tail regions on a time scale $\lesssim 4 \times 10^4$ yr and probably provide the entire energy requirements of these regions; the subsequent radiation losses provide an explanation of the change in the spectral index of the integrated emission at ~ 1 GHz.

The evidence now available is inconsistent with several of the physical models which have been proposed. The inertial and de Young & Axford models are incompatible with the upper limits on the masses of the components, as derived from the measurements of polarization, and do not account for the detailed shape of the components. Models based on a high temperature, high density ambient gas to provide the pressure needed to contain the compact components do not explain the physical alignment of the components with the central nucleus. The models most likely to provide a satisfactory explanation of the details observed seem to be those in which energy is continually transported to the components from the nucleus in the form of energetic particles or low frequency waves.

1. INTRODUCTION

The relative proximity of the powerful extragalactic radio source Cygnus A (3C 405) has made possible much more detailed investigations of its properties than for other sources of high radio luminosity. The physical scale corresponding to a given instrumental angular resolution is at least ten times smaller than for similar sources, whilst the very large flux density permits studies of the spectral distribution and polarization over a wide range of radio frequencies. Some authors (e.g. Mitton 1973) have suggested that Cygnus A cannot be regarded as typical of the powerful radio sources in that its components have considerably larger energy densities, magnetic fields and rotation measures than those of any other radio galaxy of comparable physical size. Since we know so much less about the properties of other sources, it may be premature to draw this conclusion. If the

data on Cygnus A were restricted to those available for 3C 55, 295 and 438, for example, it is doubtful whether Cygnus A would be thought to be exceptional.

High resolution maps of the total emission have already been made with the Cambridge One-Mile telescope at frequencies of 1·4, 2·7 and 5 GHz (Macdonald, Kenderdine & Neville 1968; Mitton & Ryle 1969) and of the polarized emission at 5 GHz (Mitton 1971). Information on the structure of some of the compact components has also been provided by long baseline observations at 2·7 GHz (Basart, Clarke & Kramer 1968; Miley & Wade 1971). The Cambridge 5-km telescope has now been used to map both the total and polarized emission at 5 GHz with a resolution of 2″·0 arc in right ascension and 3″·1 arc in declination. These maps show new details of the distribution of emissivity and magnetic field structure in the extensive regions of low surface brightness as well as in the two main components. A re-examination of the available interferometric data, and observations at 15 GHz (also with the 5-km telescope), have helped to define the structure in the very bright *Sf* component. A compact source coincident with the nucleus of the galaxy has also been found, giving evidence for continuing energy production.

The observations, which were made during 1973 January–March, are described in Section 2 together with the main features of the maps. The compact components are discussed in Section 3 and the spectrum in Section 4. The physical conditions needed to account for the emission in terms of the synchrotron mechanism are considered in Section 5 where the physical structure of the source is related to various theoretical models.

2. THE OBSERVATIONS AND RESULTS

2.1 *Observations*

The 5-km telescope (Ryle 1972) consists of four fixed and four moveable aerials mounted on an E–W line 4·6 km in length, so that 16 interferometer spacings are available simultaneously. In the present observations four separate 12-hr runs were made with different positions of the moveable aerials, the total of 64 spacings allowing mapping of a field 170″ arc in diameter. For observations of the polarized emission only 32 spacings were employed because no features greater than 85″ arc in extent, and having sufficient surface brightness for polarization measurements, were found in the former observations.

The flux density scale of the instrument was calibrated by assuming a 5-GHz flux density for 3C 147 of 8·2 f.u. (1 f.u. = 10^{-26} W m^{-2} Hz^{-1}), as given by Kellermann, Pauliny-Toth & Williams (1969). The first maps were made with feeds having the **E** vector in p.a. 90° and represent the distribution of I–Q. There is a close correspondence between these maps and those of I and in the remainder of this paper they will be referred to as the ' unpolarized maps ' although they have not been corrected for Q. A note is made where the consequent error exceeds one contour. The polarization was measured by means of mutually perpendicular feeds in the fixed and moving aerials. Instead of simply using p.a. 0° and 90° for U (and p.a. 45° and 135° for Q), U was determined from the mean of the observations made with the feeds of the fixed and moving aerials at position angles successively (a) 0° and 90° and (b) 90° and 0°, as shown in Fig. 1. This procedure eliminates the first-order instrumental effects, and the residual corrections (< 0·3 per cent) have been neglected. A similar method was used in the determina-

tion of Q. The sequence of feed positions shown in Fig. 1 was repeated every 200 s so that each sampling point has been corrected for instrumental polarization.

2.2 *The unpolarized maps*

A map of the distribution of unpolarized radiation is shown in Fig. 2, with equal angular scales in the two coordinates which here and elsewhere in this paper, are for epoch 1950·0. It shows the two main components together with a third component, not reported hitherto, coincident with the optical galaxy and having a flux density 0·25 per cent of the total. The aperture grading function produced a negative sidelobe response of 4 per cent at 2″ arc and a positive response of 3 per cent at 3″ arc; the maps have been corrected for these responses within 3″ arc of each of the two main compact sources. A 1 per cent grating response, at a radius of 42″ arc from the *Sf* component, arising from a small inequality in the gains at one of the positions of the moving aerials, has been removed; the corresponding response for the *Np* component was less than one contour and did not need correction.

More detailed maps of the main components are given in Figs 3 and 4, with the compact features shown on a larger scale and with increased contour interval in Fig. 5(a) and (b); the central component is shown in Fig. 6. Figs 3, 4 and 5 are

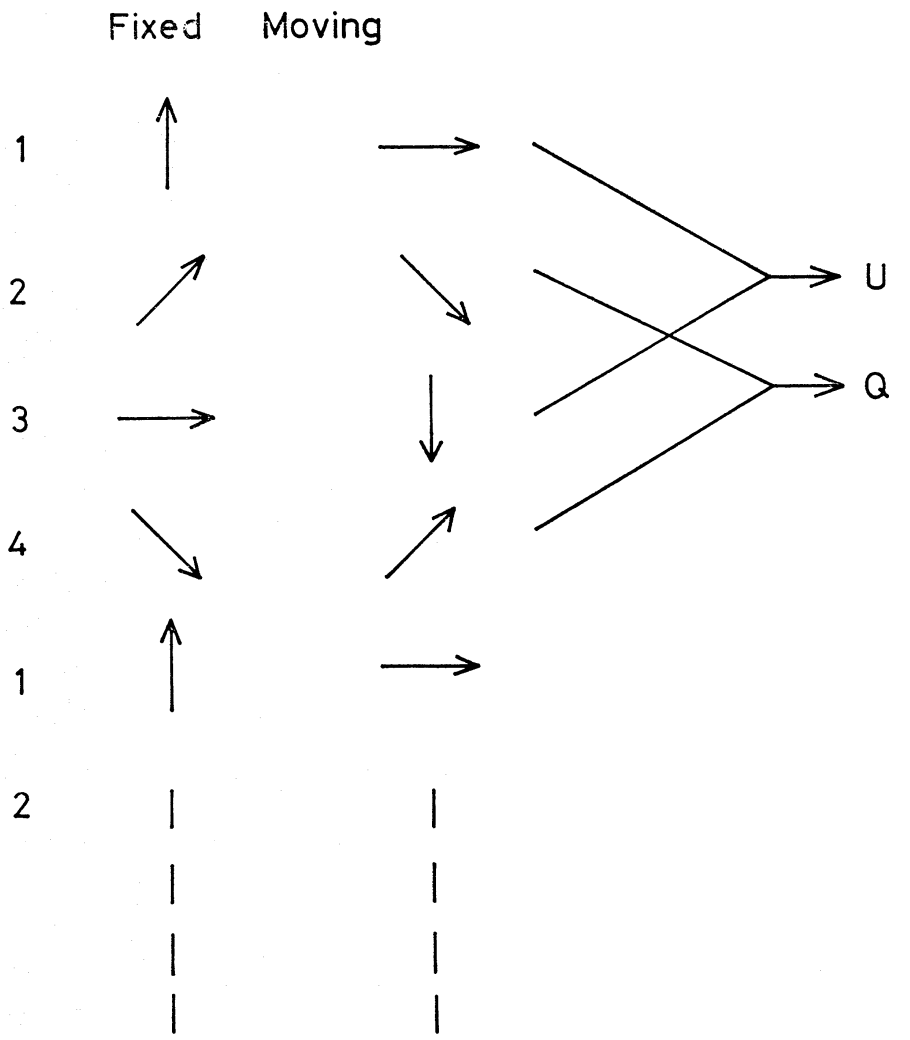

FIG. 1. *The sequence of feed position angles used to map the polarized emission.*

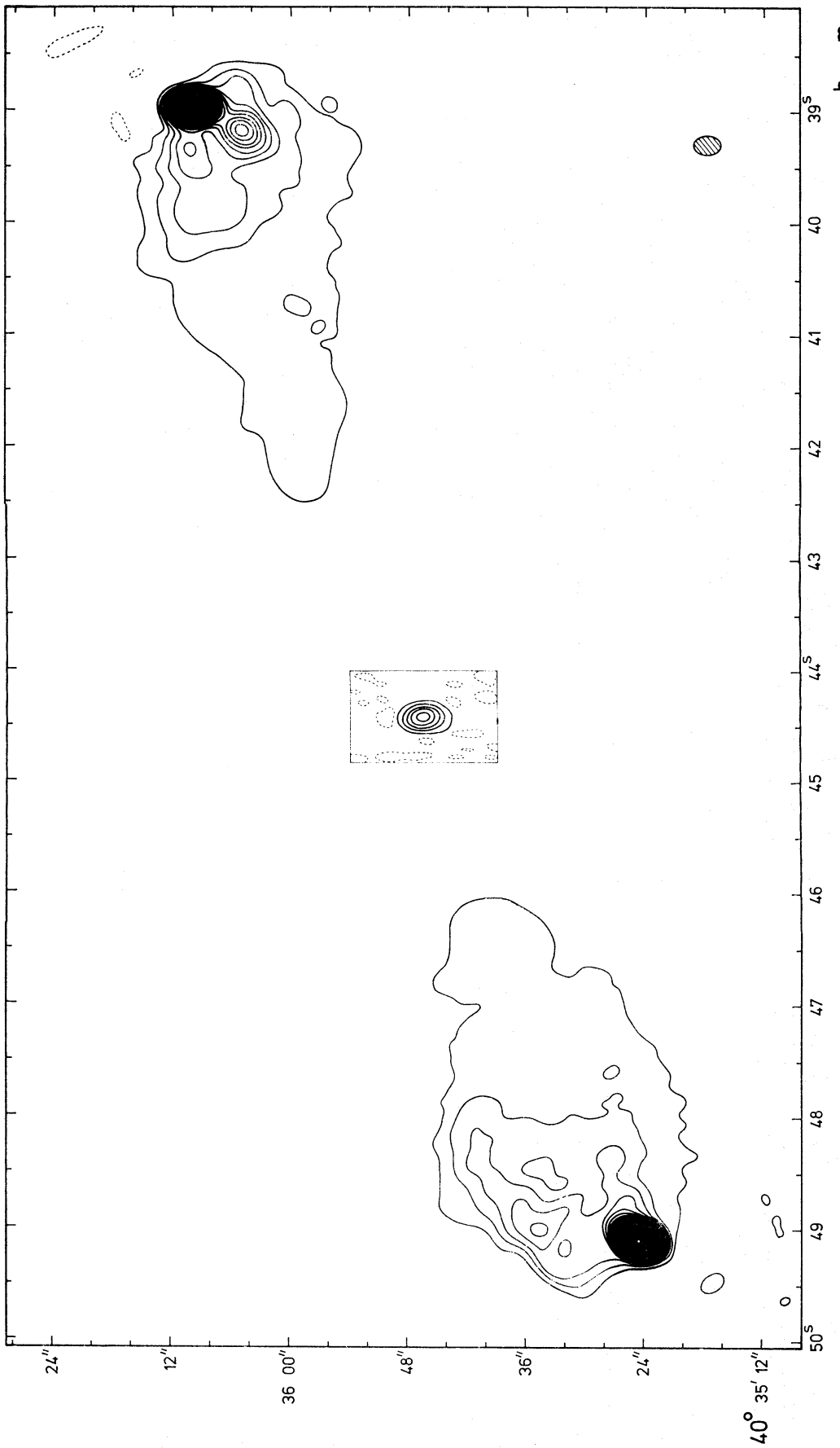

FIG. 2. *The contours of brightness temperature in Cygnus A at 5 GHz. For the two main components the contour interval is* 10^4 *K and the outermost contour represents a brightness temperature of* 0 ± 2500 *K. The solid regions in the Np and Sf component reach* 31 *and* 41 *contours respectively. The area surrounding the central component is drawn with an interval of* 2000 *K. The half-power beamwidth is indicated by the shaded ellipse.*

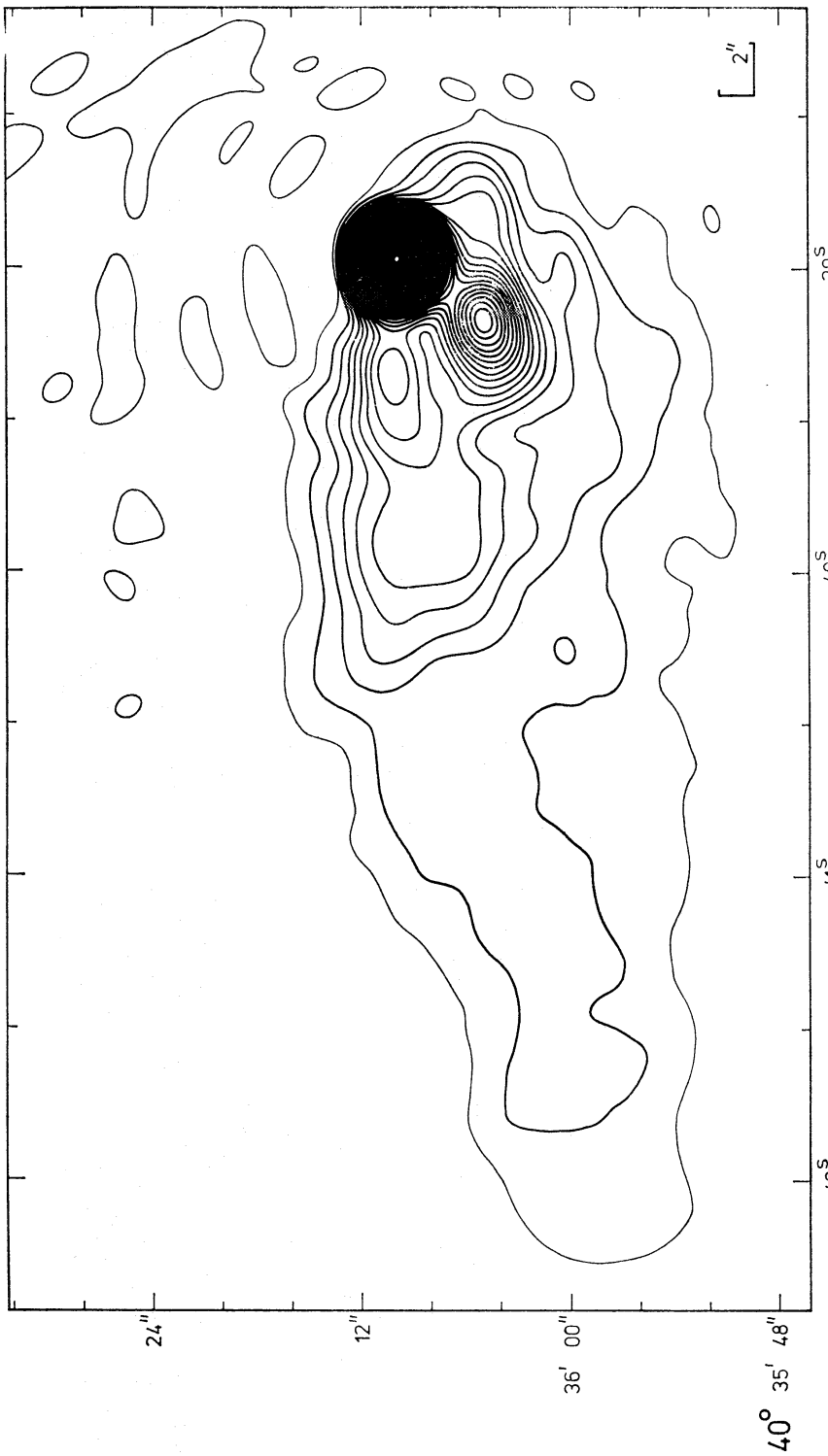

FIG. 3. *The Np component drawn with a contour interval of 5000 K. The declination scale has been compressed by a factor of 1·55 so that the beam is circular.*

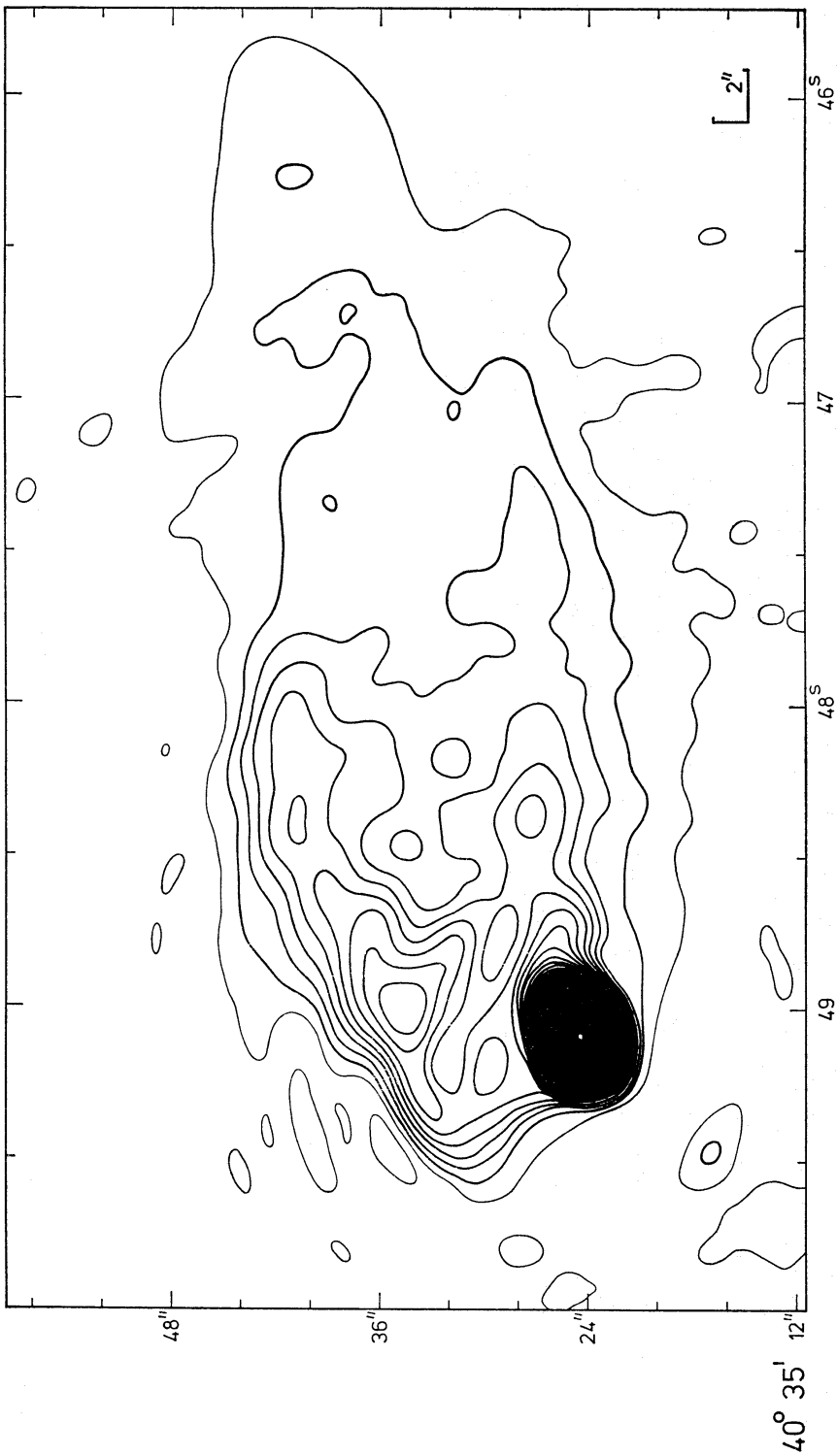

FIG. 4. *The Sf component drawn with a contour interval of* 5000 *K. As in Fig.* 3, *the declination scale has been compressed by a factor of* 1·55 *so that the beam is circular.*

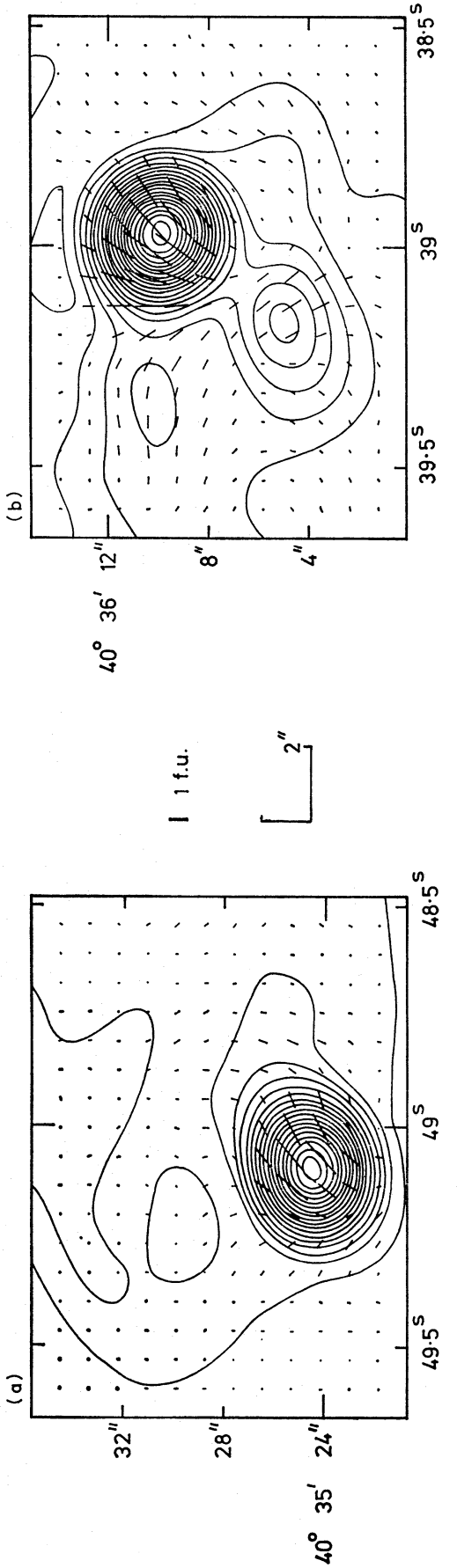

FIG. 5. *The compact features drawn with a contour interval of* $2{\cdot}5 \times 10^4$ *K and vectors showing the position angle (of the electric vector) and magnitude of the linearly polarized emission. The vertical line indicates a polarized flux of* 1 *f.u. (a) The Sf component. (b) The Np component. The letters indicate the four compact components discussed in the text.*

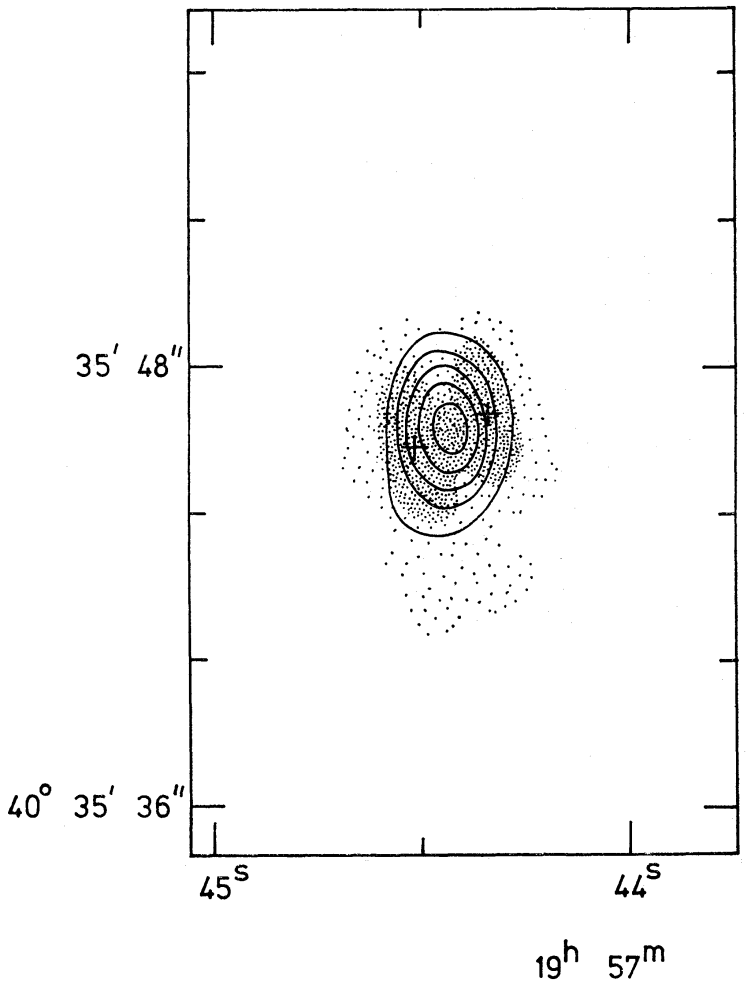

FIG. 6. *The central component drawn with a contour interval of* 2000 *K. The centres of the two optical nuclei* (*Griffin* 1963) *are also shown.*

plotted with the declination scale compressed by a factor of 1·55 so that the response of the telescope is circular. The two main components are both characterized by compact regions of very high surface brightness near the outer extremities, from which complex regions of much lower surface brightness extend towards the galaxy. As in many other sources (Harris 1974) these extensions have 'ridges' which are inclined to the axis of the system by about 20° for the *Np* component and 35° for the *Sf* component, although in the latter there is a secondary ridge much closer (10°) to the axis.

As will be discussed in Section 2.3.1, some of the regions of low surface brightness have a very large percentage polarization, and the difference between the maps presented (I–Q) and the true total intensity (I) is significant. In one region of the *Np* component ($\alpha = 19^h\,57^m\,41^s$, $\delta = 40°\,36'\,00''$) the correction corresponds to about one contour interval in Fig. 3. In the same way the strong polarization in and around the compact component C (Fig. 5(b)) increases the brightness of the minimum between components A and C.

In describing features whose angular extents are comparable with or smaller than the resolution of the instrument a gaussian model has been used; the angular diameters quoted represent the full width between the half-intensity points. The compact structure in the *Np* component (Figs 3 and 5(b)) comprises a main

source (A) with flux density of 38 f.u. whose angular diameter as measured from the map is 1″·5 × 1″·9 arc; a second, elongated source (B) with a flux density of 8 f.u., 2″·0 × 0″·9 arc in diameter and 5″·6 away along p.a. 155°; and a third sub-component (C) of ~2 f.u., 4″·3 arc away from A along p.a. 90°. The source model proposed by Miley & Wade (1971) included two northerly components of size 1″·0 aligned in p.a. 130° which may be identified with our A and B.

The *Sf* component (Figs 4 and 5(a)) contains the most intense sub-component, with a diameter of 2″·0 arc in p.a. 122° and 1″·5 arc in p.a. 32° and a flux density of 60 f.u. Miley & Wade were not able to fit a model for this sub-component but they suggested that it was a double or multiple object with component sizes 0″·5 to 0″·6 arc. The structure is discussed further in Section 3.

The position of the central component coincides with the mid-point between the two optical 'nuclei' within the limits of accuracy of the relative positions (Fig. 6). Its small angular size (< 1″·0 arc) suggests that the radio emission is not associated with either of the optical maxima. No radio emission is detectable from the envelope of the galaxy.

A line through the intense sources (A and D) in the *Np* and *Sf* components passes within 1″·0 arc of the central source, indicating the remarkable precision with which the compact regions lie in opposite directions from the nucleus. Any transverse component of velocity is therefore less than 2 per cent of their radial velocity. The angular distances of these components from the nucleus in Fig. 2 are 67″ arc (*Np*) and 57″ arc (*Sf*), but it is clear from the complex nature of the components that the apparent distances from the centre will depend strongly on the resolving power of the instrument, as has been discussed by Mitton & Ryle (1969).

The details of the source components are summarized in Table I, where the angular measures have been converted into physical scales on the assumption of an Einstein–de Sitter world model with a value of Hubble's constant of 50 km s^{-1} Mpc^{-1}. Since $z = 0{\cdot}0561$ (Schmidt 1965), the distance of Cygnus A is 323 Mpc and 1″ arc corresponds to 1·5 kpc.

The total measured flux density is some 16 per cent greater than that given by Kellermann, Pauliny–Toth & Williams (1969) for 5 GHz, but is in good agreement with the spectrum fitted by Mitton & Ryle (1969) which takes account of observations at a number of adjacent frequencies.

2.3 *The polarized emission*

Maps of the linearly polarized emission are shown in Figs 7 and 8; the lowest contour in each of the unpolarized maps is included to indicate the extent of the components. The polarization is also given in Fig. 5(a) and (b) with lower sensitivity, to show that structure within the compact regions. It can be seen that there is a very marked difference between the two components; the whole of the *Np* component exhibits areas of strong polarization whereas the polarization in the *Sf* component is largely restricted to the area of the compact source. We now consider the components separately:

2.3.1 *The Np component.* Each of the three compact sources A, B and C can be distinguished in the map of the polarized emission, and their percentage polarizations and position angles are listed in Table I. The polarization from the tail exhibits variations in magnitude and position angle on a scale of 1″ to 2″ arc which do not appear to be associated with corresponding variations in the unpolarized

TABLE I

Component	Flux density f.u.	Position 1950·0 h	m	s	°	′	″	Angular size (″ arc)	Linear size (kpc)	Separation from central source (″ arc)	(kpc)	Peak percentage polarization	Position angle (°)
A	38	19	57	38·97	40	36	10·0	1·5 × 1·9	2·2 × 2·8	67	98	12	145
B	8	19	57	39·17	40	36	05·0	2·0 × 0·9	3·0 × 1·3	63	93	14	30
C	~2	19	57	39·34	40	36	10·1	~2	~3	63	93	20	90
Np tail	164	—			—			22 × 11	33 × 16	—	—	—	—
D	60	19	57	49·09	40	35	24·6	1·5 × 2·0	2·2 × 3·0	57	8	7	130
Sf tail	160	—			—			22 × 13	33 × 19	—	—	—	—
Central component	1·1	19	57	44·43	40	35	46·3	< 1	< 1·5	—	—	< 5	—

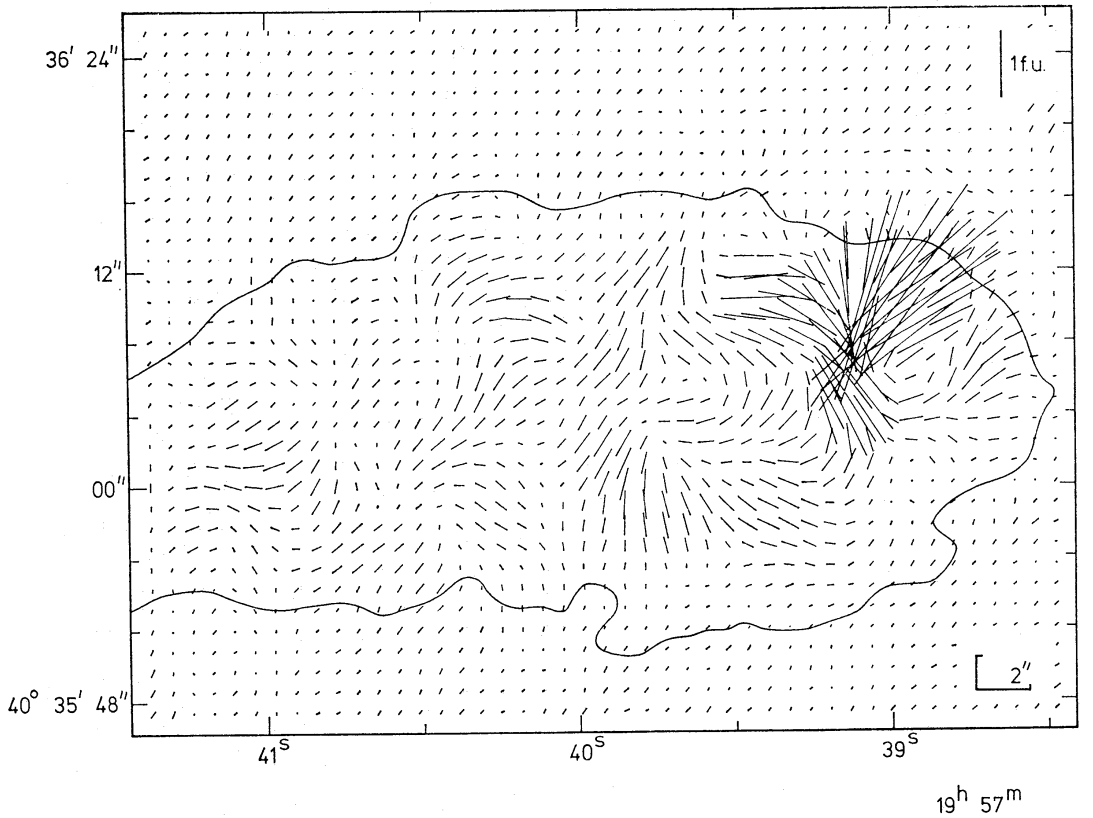

FIG. 7. *The polarized emission from the Np component. The lines indicate the direction of the electric vector. The first contour of the unpolarized emission from Fig.* 3 *is shown.*

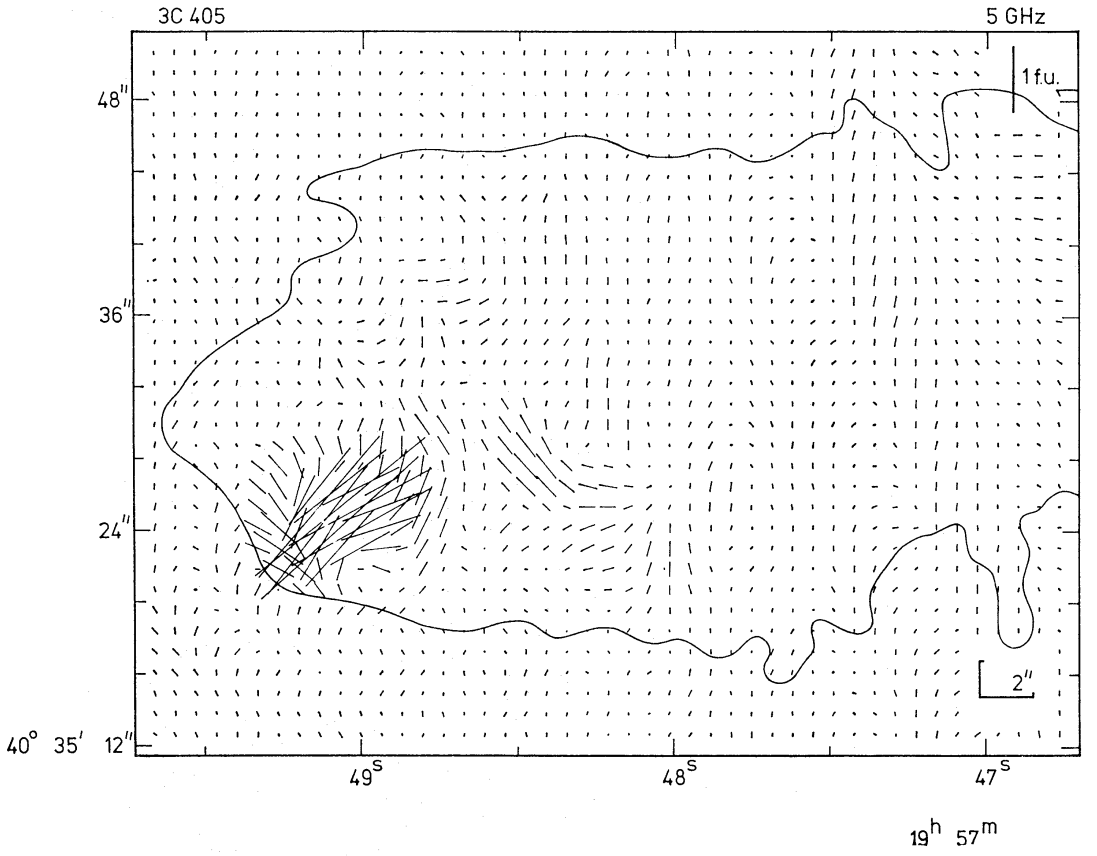

FIG. 8. *The polarized emission from the Sf component. The first contour of the unpolarized emission from Fig.* 4 *is also shown.*

emission. Over parts of the tail the polarization has values of ~25 per cent, much higher than in the compact regions. Since the maximum polarization possible from the synchrotron mechanism is only 75 per cent it is therefore unlikely that the true scale of the polarized structure in the tail can be much smaller than that apparent on the map. When integrated over the whole of the *Np* component the polarization is $1{\cdot}5 \pm 0{\cdot}3$ per cent in p.a. $152^\circ \pm 3$.

2.3.2 *The Sf component.* The maximum polarization coincides with the compact source but its magnitude is only 7 per cent. The polarization from one region of the tail attains a value of 18 per cent, but over most of the tail is less than 5 per cent. The marked difference between the *Np* and *Sf* components may be associated with the larger rotation measure derived for the *Sf* component from previous observations (Schraml & Turlo 1967; Mitton 1971); the great complexity of the polarization structure, however, and the possibility of differential rotation across the source, make the interpretation hazardous until high resolution measurements are available at another frequency.

The net polarization found by integrating over the whole of the *Sf* component is $1{\cdot}0 \pm 0{\cdot}3$ per cent in p.a. $139^\circ \pm 3$.

2.3.3 *The central component.* An upper limit of 5 per cent can be set on the polarization of the central component.

2.3.4 *The total polarization.* The integrated polarizations found for both the *Np* and *Sf* components are lower than those reported by Mitton (1971). The integrated polarization for the whole source ($1{\cdot}2 \pm 0{\cdot}3$ per cent in p.a. $147^\circ \pm 3$) is also lower than his figure and is in better agreement with the results at adjacent frequencies (Hollinger, Mayer & Menella 1964; Gol'nev & Soboleva 1965).

3. THE COMPACT SOURCES

3.1 *The compact sources in the Np and Sf components*

In this section we examine evidence for structure in the compact sources on a scale smaller than that revealed by the observations of Section 2. The volume emissivity from any such features might imply an energy density greater than that derived (Section 5.1) for the components A, B, C and D and hence present an even more severe containment problem. Miley & Wade have used larger baselines ($1{\cdot}0$ to $3{\cdot}2 \times 10^5$ λ) at 2·7 GHz than in the present 5 GHz observations (up to $7{\cdot}6 \times 10^4$ λ), although for a limited range of position angles and baselines. For the *Np* component a plot of fringe visibility, combining both the present 5 GHz results and those of Miley & Wade, in position angles parallel and perpendicular to the line joining A and B, indicates that the component sizes derived from the maps are consistent with all the observations. In the case of the *Sf* component, however, the visibility predicted from the $1''{\cdot}5 \times 2''{\cdot}0$ arc gaussian source model falls significantly below that found by Miley & Wade with a baseline of 3×10^5 λ. It is important to establish whether this result implies, as Miley & Wade have suggested, the existence of several compact regions of high surface brightness or whether it is better attributed to some other distribution.

In order to investigate this point, further observations of higher resolving power have been made, using 15·4 GHz receivers temporarily installed in three of the 5-km aerials to study tropospheric irregularities (Hinder & Ryle 1971). During these experiments the opportunity was taken to observe Cygnus A at baselines of $1{\cdot}0$ and $2{\cdot}2 \times 10^5$ λ with full coverage in position angle. The *Np* component showed

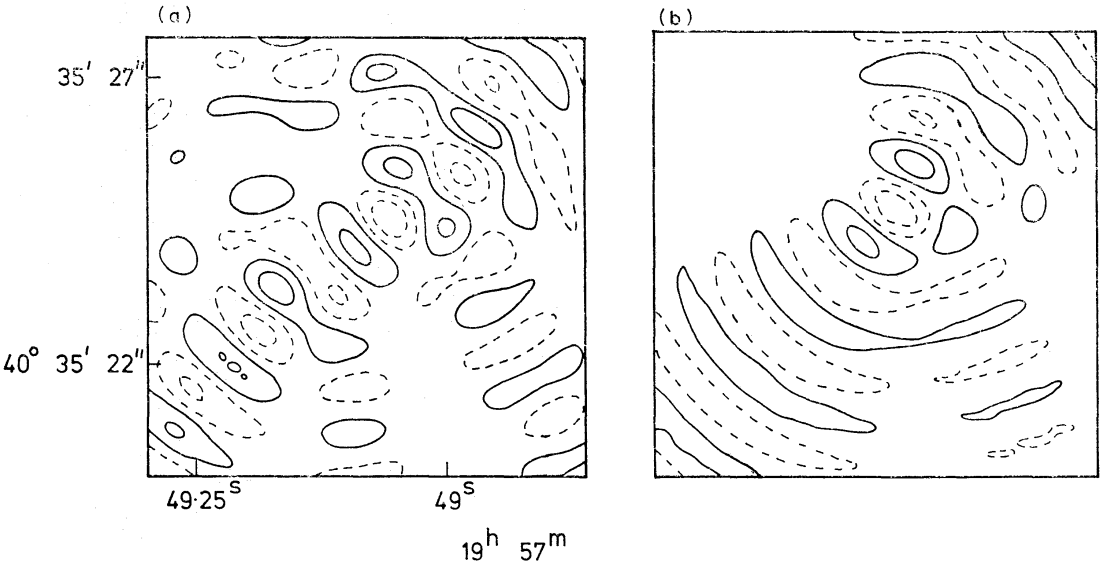

FIG. 9. (*a*) *The map obtained at* 15·4 *GHz using a spacing of* $2{\cdot}2 \times 10^5$ λ. (*b*) *The corresponding map calculated by convolving the source model shown in Fig.* 10 *with the instrumental response.*

no amplitude greater than $S_{15} = 1{\cdot}4$ f.u., corresponding to a value of $S_5 = 3{\cdot}4$ f.u. on the assumption of a spectral index of 0·8, and indicated that this component is well represented by the structure apparent on the 5-GHz map. The corresponding results for the *Sf* component are of great interest and the map corresponding to the $2{\cdot}2 \times 10^5$ λ baseline is shown in Fig. 9(a). The response for a 12-hr observation is a J_0 Bessel function, so that an unresolved source would produce a central maximum having a width to half-intensity of 0″·4 arc, surrounded by rings of amplitude −40 per cent and +30 per cent etc. In the projection used in the map of Fig. 9(a) these rings would be circular. The actual map is quite different and reveals a series of elongated ridges. Such a configuration can most simply be explained by a linear structure running nearly perpendicular to the major axis of the 5-GHz source. The distribution and observed flux density can both be accounted for by a model in which the outer edge of the component is sharply truncated. Various models of the component, having distributions corresponding to half an elliptical gaussian $3''{\cdot}4 \times 1''{\cdot}1$ arc but with different forms of the truncation of the outer (*Sf*) edge, have been convolved with the response function of the telescope. The range of models was such as to display the effects of variation of (a) the abruptness of the truncation, and (b) the position angle, ϕ, of the truncation. One of the models which provides a map (Fig. 9(b)) in good agreement with the observations is illustrated in Fig. 10. By examining a wide range of models it may be concluded that (a) the truncation of the brightness of the component is very sharp and may be fitted by a gaussian of width β to half-intensity $< 0''{\cdot}25$ arc, and (b) $\phi \sim 35°$, a direction close to the normals to both the axis (p.a. 122°) of the *Sf* component as measured from the 5-GHz map and the line joining the main sub-components A and D (p.a. 111°). Such a model is consistent with the observations of Miley & Wade and it follows that there is no need to assume, with them, the existence of very compact sub-components of high surface brightness.

If it is supposed that the distribution of Fig. 10 has rotational symmetry about the sub-component axis (p.a. 125°) then the upper limit on β imposes the important

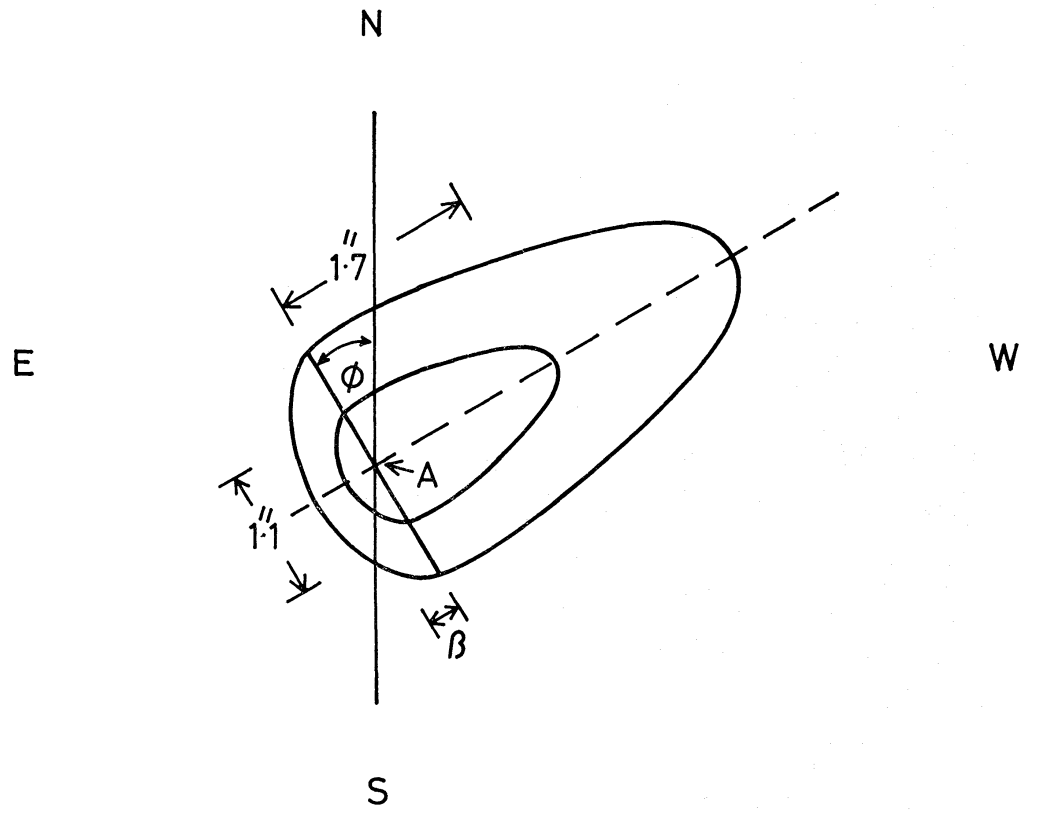

FIG. 10. *The source model for the Sf component derived from the 15·4 GHz observations. A represents the peak brightness and the contours are drawn at 50 per cent and 10 per cent of this value. The half width (β) and the position angle (φ) of the truncation were varied to determine the range of values consistent with the observations.*

restriction that the angle between the sub-component axis and the line of sight is $90° \pm 15°$. In view of the closeness of the sub-component and source axes as projected on the sky, it seems likely that the source axis itself lies within $90° \pm 25°$ of the line of sight. It may be that the structure of the *Np* sub-component A is in fact similar to the model considered, the difference in this case being that the line of sight does not lie in the plane of truncation and hence the outer cut-off is much less abrupt than in the *Sf* sub-component.

This new evidence on the form of the compact sub-components is of importance in relation to some of the physical models, as will be discussed in Section 5.

3.2 *The central source*

The limit on the angular size of the central source corresponds to a physical size $< 1·5$ kpc. The optical (Griffin 1963) and radio positions are accurate enough to place this source between the two optical maxima and the extent of the radio source is small enough to indicate that there is no detectable radio emission coming from these maxima. The position angle of the line joining the centres of these optical condensations is 115° (Baade & Minkowski 1954) which is very close to that of the radio source axis (111°) suggesting that they may be associated with the ejection of the radio components. Alternatively the apparent double nature of the nucleus could be the result of obscuration by a dust lane as in the case of NGC 5128; alignment of the two axes would then suggest that the ejection of the radio components took place along the rotation axis of the galaxy, in agreement with some

source models. Observations of the nuclear region in the infra-red might enable a distinction to be made between these possibilities and also provide further information on the central source of radio emission. No spectral information is available for the radio emission, but the total radio power is likely to be at least $\sim 10^{42}$ erg s^{-1}, a figure which may be compared with the value of $\sim 10^{45}$ erg s^{-1} derived by Mitton & Mitton (1972) for the optical line emission from the whole nuclear region (5″ arc in diameter).

4. THE RADIO SPECTRUM

The integrated spectrum of Cygnus A is well determined but as yet there is only limited information on the spectra of the individual components. Earlier observations with a resolution of 12″ × 19″ arc (Mitton & Ryle 1969) showed, however, that the spectra of the extended features are significantly steeper than those of the regions of high surface brightness. With the more detailed information on the 5-GHz structure now available it is possible to improve this analysis and establish more accurate values for the spectral indices α (defined as $S \propto \nu^{-\alpha}$) of the compact components. For both the *Np* and *Sf* components $\alpha = 0{\cdot}8 \pm 0{\cdot}1$, in contrast to the value of $\alpha = 1{\cdot}2$ for each of the extended features (Mitton & Ryle 1969).

It is important to obtain spectral information on the compact components at lower frequencies in order to investigate whether synchrotron self-absorption occurs and hence to place limits on the magnetic field strength. The large reduction in the integrated flux for $\nu < 25$ MHz (e.g. Mitton & Ryle 1969) cannot be due solely to this cause, since it represents a reduction greater than the total flux in the compact sources (assuming them to have $\alpha = 0{\cdot}8$ throughout the radio frequency range), and must instead be attributed either to synchrotron self-absorption in the extended features or to free-free absorption in the Galaxy. There is also a progressive change in the spectral index of the integrated emission near 1 GHz which, although of too great a magnitude to be due entirely to self-absorption in the very compact components, might have a contribution from such effects. A determination of the flux density of the compact components at a low frequency is therefore of great interest. The scattering effects of the interstellar medium (Readhead & Hewish 1972) are a serious handicap, since the apparent angular size of a source is increased at low frequencies and it may then become impossible to distinguish between the contributions from the compact sub-components and the more extended features. The apparent angular size of a source of actual angular size θ is given by $(\theta^2 + \theta_s^2)^{1/2}$ where θ_s is the scattering angle. θ_s is proportional to λ^2 and depends on the distance through the Galaxy in the direction of the source. For a frequency of 81·5 MHz and the galactic coordinates of Cygnus A, $\theta_s \gtrsim 1''{\cdot}5$ arc. This result shows that the interferometric measurements by Slee & Wraith (1967) at 38 MHz with a baseline of 16 200 λ are dominated by the effect of interstellar scattering so that it is difficult to derive the flux densities of the compact sources.

Interstellar scattering is less important for the observations by Rowson (1963) at 158 MHz with a baseline of 61 100 λ and Erickson *et al.* (1972) at 121·6 MHz with a baseline of 92 000 λ. Rowson's data have been compared with the results obtained by the 5-km telescope over the same range of baseline and position angle. An absolute calibration of the scale of flux density was not available for the 158 MHz

observations but a compact source having an apparent diameter $\sim 2''{\cdot}5$ arc is revealed in each component. That in the *Np* component has a flux density of at least 215 f.u. and that in the *Sf* component a flux density of at least 340 f.u. The measured angular sizes are close to those expected from interstellar scattering and, although the estimated flux densities are smaller than the figures obtained by extrapolation of the high frequency data (630 and 950 f.u. respectively), the results suggest that synchrotron self-absorption is not important for $\nu > 158$ MHz, even in the compact regions.

The mean spectral index of the extended features decreases progressively from 1·2 at 2·7 GHz to 0·8 at 100 MHz. It is unlikely that this decrease can be explained in terms of synchrotron self-absorption occurring successively in different parts of the extended features. As suggested by Bridle (1967) the turnover at 25 MHz is much more likely to be due to free-free absorption in the Galaxy.

5. THE PHYSICAL CONDITIONS WITHIN THE SOURCE

5.1 *Energy requirements*

The minimum energy requirements $U_{\min}$ based on the synchrotron mechanism, and making no allowance for the possible presence of high energy protons, are shown for the different source components in Table II; the Table also gives the corresponding values for the magnetic field and radiation lifetimes of 5 GHz electrons. The cut-off frequencies associated with synchrotron self-absorption are less than 60 MHz even for the most compact components, a result consistent with the observations; the cut-off at $\nu \sim 25$ MHz is more likely to be due to galactic free-free absorption as already discussed.

TABLE II

Component	$U_{\min}$ (10^{56} erg)	B_{eq} (10^{-4} G)	Lifetime of 5 GHz electrons (10^4 yr)
A	32	2·9	5
B	8	2·6	6
Np tail	2900	1·2	18
D	38	3·4	4
Sf tail	3300	1·1	21

There is no evidence for a break in the spectrum of the compact components which could be attributed to radiation losses at frequencies less than 5 GHz; the particles must therefore remain in these regions for less than 4×10^4 yr. In fact the sizes of the compact components are of the order of 6×10^3 light-years and so the particles must diffuse out of them rather quickly. The rate of supply of energy to the compact regions must therefore be 10^{45}–10^{46} erg s^{-1}. The minimum energy requirements of the tails, assuuming equipartition, could therefore be supplied by the particles leaving the compact regions if this rate has continued for 10^6–10^7 yr. It should be noted, however, that for the upper age limit the synchrotron losses would lead to a break in the spectrum at $\nu \ll 1$ GHz. Either the age of the source

must be closer to 10^6 yr or the assumption of equipartition is invalid. In any case it appears that continuing acceleration of electrons must take place within the compact heads; how this might occur within the context of different models will be discussed in Section 5.3.

5.2 *The gas density estimated from the polarization measurements*

The fact that polarized emission is observed in the brightest sub-components sets useful limits to the gas density within these.

5.2.1 *The Sf component.* Most of the polarized emission is associated with the head of the component and it is likely that this provides the major contribution to polarization at all frequencies. Thus at high frequencies, at which there is little Faraday depolarization, the overall percentage polarization of the *Sf* component (7·5 per cent, e.g. Mitton 1971) can be attributed to the intrinsic polarization of the compact region which then amounts to 25 per cent of the intensity of the compact head. If the reduction from the theoretical maximum polarization of about 75 per cent is due to the superposition of regions with randomly distributed field directions, it is evident that there can only be a very small number of such regions, ~ 10, within the compact head. The scale size of these regions is then ~ 1 kpc.

At 5 GHz the polarization is considerably smaller, suggesting that Faraday depolarization is important at this frequency. Fitting a depolarization law of the form $\sin(RM\lambda^2)/RM\lambda^2$ to the observations gives a rotation measure within each cell of ~ 700 rad m^{-2}, and for the equipartition value for the field leads to an electron density $N_e \sim 3 \times 10^{-3}$ cm^{-3}.

The polarization visible in the tail shows structure on a scale equal to the instrumental resolution, and it is possible that the small percentage (< 5 per cent) over most of the tail is simply due to a turbulent cell size smaller than that corresponding to the beam. For a cell size of $\sim 0{\cdot}5$ kpc the number along the line of sight and within the beam would be ~ 400 so that the expected polarization would be ~ 2 per cent. If the cell size were larger than this, and the small percentage were attributed to Faraday depolarization, typical values of $N_e \sim 5 \times 10^{-3}$ cm^{-3} are found.

5.2.2 *The Np component.* Since much of the polarized emission here originates in the complex tail region, it is difficult to make use of the measurements of integrated polarized emission at other frequencies. The strong 5 GHz polarization found in the compact components A and B (12 and 14 per cent) indicates that the scale size of any cell structure must again be $\gtrsim 1$ kpc, and that, with the equipartition magnetic field, the electron density within these components cannot exceed $N_e \sim 3 \times 10^{-3}$ cm^{-3}.

The tail of the *Np* component exhibits polarization having an angular structure comparable with the intrumental resolution, but it is much stronger than that in the *Sf* component. Assuming that the lateral scale of structure apparent on the map also occurs along each line of sight, the observed polarization implies a cell size $\sim 2{\cdot}5$ kpc; the limits which can be set on Faraday depolarization imply that $N_e \lesssim 10^{-3}$ cm^{-3}.

It is possible that the apparent difference in the scale sizes of the magnetic field structure in the *Np* and *Sf* components is associated with the large rotation measure derived from the integrated polarization of the *Sf* component (Schraml & Turlo 1967). A large gradient of rotation measure across the *Sf* component due to an intervening medium might introduce sufficient differential rotation across the

instrumental beamwidth to reduce the polarization. The models proposed to account for the asymmetry in rotation measure in terms of an extensive halo around the galaxy (Slysh 1965) require that the angle between the source axis and the line of sight is small which, as shown in Section 3.1, seems unlikely.

Whatever the explanation for this asymmetry, there is little doubt that the compact components and the extended tails have a magnetic field structure with scale size 0·5–3 kpc, and that the electron density in all regions of the source has values $N_e \lesssim 3 \times 10^{-3}$ cm^{-3}.

5.3 *Source models*

The present observations provide severe tests for several of the more plausible radio source models. The reader is referred to the papers by Longair, Ryle & Scheuer (1973), Gull & Northover (1973) and Scheuer (1974) for more complete descriptions of the physical details of these models.

5.3.1 *Inertial and de Young and Axford models.* Some models require high densities of cold matter inside the source components. In the inertial models, the source components remain compact because the relativistic particles and field are tied to sufficient cold matter to reduce the free expansion velocity of the plasma cloud. The necessary kinetic energy of the cold matter is $(D/d)^2$ times the internal energy being confined, where d and D are respectively the component size and distance from the galaxy; minimum values for the various components are listed in Table III. Lower limits to the masses and matter densities within the compact

TABLE III

(*a*) *Inertial confinement*

Component	Kinetic energy (10^{60} erg)	Mass (10^{41} g)	Matter density (cm^{-3})	Emission measure (cm^{-6} pc)
A	5	11	2	7000
B	2	4	2	9000
D	5	12	2	10 000

(*b*) *De Young & Axford confinement*

Component	Kinetic energy (10^{58} erg)	Mass (10^{39} g)	Matter density (10^{-2} cm^{-3})	Emission measure (cm^{-6} pc)
A	9	20	3	2
B	3	6	3	2
D	10	22	4	3

heads have been derived by taking the highest permissible velocities for the components, *viz.* 0·1 c (Mackay 1973). It is evident that the particle densities required (~ 2 cm^{-3}) are much higher than the estimates from the polarization data discussed above ($N_e \sim 3 \times 10^{-3}$ cm^{-3}). Furthermore the expected emission measures are in excess of those found by optical observations of the regions of the compact components (Longair *et al.* 1973).

In the ram-pressure model (de Young & Axford 1967), confinement is effected by the deceleration of the component as a whole which holds the relativistic matter against the boundary between the intergalactic gas and the component. The kinetic energy requirements in this model are $(D/d)\ U_{\min}$ for the compact components and are listed in Table III(b) together with estimates of the particle densities

assuming $v = 0{\cdot}1$ c. The particle densities are much reduced ($N_e \sim 4 \times 10^{-2}$ cm^{-3}) although they still exceed the estimates of Section 5.2 by an order of magnitude.

The discussion of Section 5.2 considered only models in which the components consisted of random superpositions of regions of uniform field. It has been pointed out by Scheuer (1967) that if such a random field is sheared, such that there are many reversals of field direction within each cell, the depolarization is greatly reduced, so that larger values of N_e could exist. As Longair, Ryle & Scheuer pointed out the gryo-radii of the particles sets a limit to the minimum scale of the folded field, and this is sufficient to eliminate the possibility of densities as high as those required in the inertial models, but if such a geometry did exist it would be possible to accept a de Young & Axford model. The optical determination of emission measure from the compact components should eventually allow a test to be made of this possibility but at present the limits are not good enough (see Table III(b)).

The variant of the de Young & Axford model discussed by Mills & Sturrock (1970) in which the magnetic field is well aligned in the tail region seems inconsistent with the observed turbulent polarization structure in this region of the north component, and the absence of polarization in the south tail.

The above discussion is also relevant to the containment models which suppose that energy is continually supplied to source components containing cold matter, such as the ' kinetic energy ' model described by Longair, Ryle & Scheuer. Perhaps the most serious criticism of models which require large amounts of cold diffuse matter relates to the difficulty in understanding how so much matter could accumulate in the compact components.

5.3.2 *Models involving the ejection of compact objects.* Models in which discrete energy sources such as massive objects, quasi-pulsars, etc., are ejected from galactic nuclei have been outlined by Burbidge (1967). A possible scheme for ejecting such objects in opposite directions from galactic nuclei has been described by Saslaw, Vaaltonen & Aarseth (private communication). Because of the compactness of the outer components such models require the ejection of single massive objects since the probability of ejecting a number of components in the same direction seems very small. The minimum energy requirements imply that the rest masses of the components are at least $10^5 M_\odot$ and, since the ages of the sources are at least 10^6 yr, it is probable that whatever their origin, such massive objects will have evolved into black holes. It is not clear whether there are mechanisms by which such black holes travelling through the rarefied intergalactic gas could release the necessary energy over relevant time scales.

5.3.3 *The Bubble model of Gull & Northover.* Gull & Northover (1973) have recently proposed that even the most compact components of Cygnus A could be contained by the thermal pressure of a hot dense gas ($T \sim 2 \times 10^9$ K; $N_e \sim 10^{-2}$ cm^{-3}) surrounding a massive galaxy. There is no necessity for any non-relativistic particles inside the components, although there is no reason why cold matter should not be there. A feature of the model is the very high ambient gas density which, even in the presence of a very weak field, could cause considerable Faraday rotation since the path length through the gas is long. If there are fluctuations in the magnetic field in the intra-cluster medium on a scale $\ll 3$ kpc, these could produce the observed depolarization in the source in the absence of Faraday rotation within the components. The velocities of the components are always small in this model (~ 350 km s^{-1}) and so the age of the source must be $\sim 10^8$ yr. The present observations then pose considerable problems for the model since the synchrotron lifetimes

for 5 GHz particles in the heads and tails of the source components are only 4×10^4 yr and 2×10^5 yr respectively (Section 5.1). The avoid this difficulty Gull & Northover proposed that the ' hot spots ' were regions of enhanced field within a reservoir of particles in a much weaker field. The reservoir must, however, include regions of the tail where the derived equipartition field is far too great to allow lifetimes of $\sim 10^8$ yr. Gull & Northover also suggest that particles may be accelerated continuously from a turbulent field maintained by the bulk motion of the bubble, but whatever the field strength the total kinetic energy available is insufficient to maintain the emission for the necessary time.

A further feature which has no immediate explanation in their model is the very precise alignment of the two main compact components with the central source; the line joining A and D passing within 1″ arc of the central source. In the vortex model of the ' hot spots ' a typical deviation of 5″ arc would be expected. These difficulties may not exclude the bubble model, but modifications to the original version seem necessary.

5.3.4 *Continuous flow models.* In these models, the compact components are continuously supplied by a beam which may consist of strong electromagnetic waves or relativistic particles. Such a model employing strong waves has been discussed by Rees (1971) and the dynamics of this general class of model have been considered by Scheuer (1974). The beam sweeps back the intergalactic gas, the particles are accelerated or randomized at the interface between the beam and the ambient gas, and then escape rapidly from this region since there is no restraining pressure or internal cold matter. Scheuer (1974) has shown that the escape of particles results in a cigar-shaped cavity whose shape may be modified by the

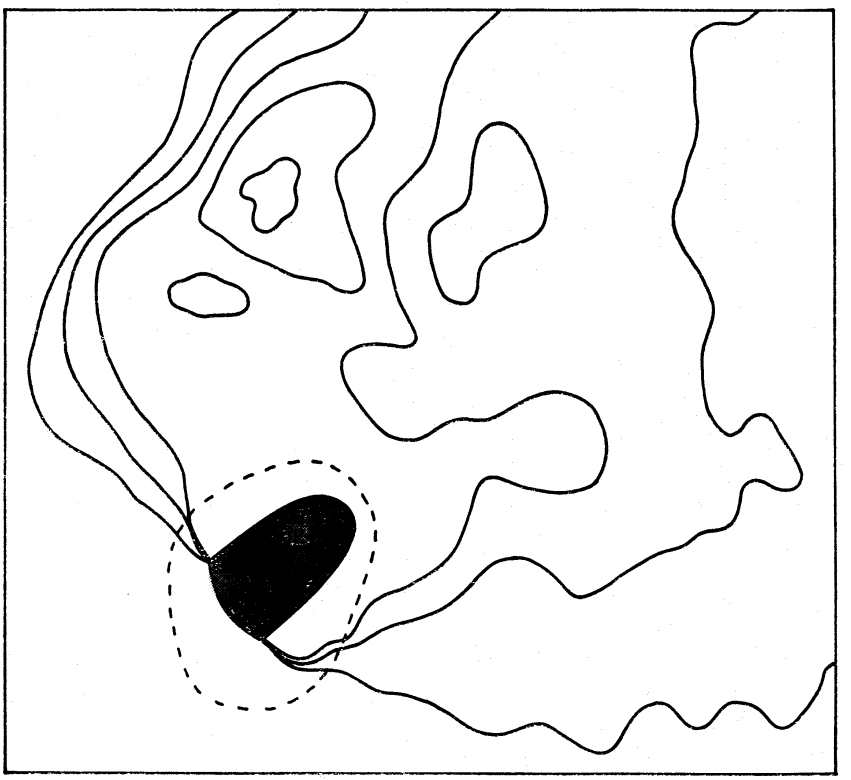

FIG. 11. *Sketch map showing the approximate extent of the Sf head in relation to the extensive tail. The curvature of the outer edge corresponds to the maximum permitted by the 15·4 GHz observations. The dotted line indicates the extent of the compact source on the* 5 GHz map.

presence of a hot intergalactic gas. In this model the hot spots observed in both components are identified with points at which the beam encounters the intergalactic gas. The radio structure of the compact southern component shown in Fig. 11 is in excellent agreement with this model, the sharp leading edge being identified with the interface between the beam and the intergalactic gas. The rapid diffusion of the particles from this region is consistent with the spectral data discussed in Section 5.1.

The present observations can be used to derive a self-consistent model of this type for the whole source. In the simple model of the dynamics there is no thermal matter within either the compact regions or the extensive tails. However, it is quite possible that, because of the incidence of instabilities at the surface, intergalactic gas mixes with the relativistic gas in the tail, and the magnetic field is amplified to equipartition values. Taking the particle densities estimated from the polarization data, $N_e \sim 10^{-3}$ cm^{-3}, to be typical of the intergalactic gas density, ram pressure balance at the head requires $\rho V^2 = \frac{1}{3}U$ and the velocity of the component through the intergalactic gas would be $\sim 0{\cdot}04$ c. The age of the source is then 10^7 yr, although the accelerated particles in the head need spend no more than the light travel time of $\sim 10^4$ yr within the compact heads. In some versions of this model the extensive tails are in pressure equilibrium with a hot intergalactic gas. Equating NkT to the internal pressure of the tail, we find $T \sim 10^9$ K, which is of the order of the equilibrium temperature within a rich cluster as estimated by Gull and Northover. The density does not, however, have the high values considered in their model and the X-ray emission would be some 100 times weaker.

The models based on a continuous flow of low-frequency radiation or relativistic particles from a continuing source of energy within the nucleus of the galaxy provide a more satisfactory explanation for the observations of Cygnus A than any of the other models proposed.

6. CONCLUSIONS

The following features of the new high-resolution observations of Cygnus A seem to be particularly significant.

(i) The maps show much fine structure in both the *Np* and *Sf* components. Both contain very compact components and both have ridges of emission whose directions are displaced from the source axis. A central source coincident with the nucleus of the optical galaxy has been found.

(ii) The polarization maps reveal high percentages throughout much of the source, both in the compact components and in the extensive tails. This result, together with the 15·4 GHz observations, indicates that there is unlikely to be very much structure on a smaller scale than that indicated on the maps. In particular there do not appear to be smaller components of even larger surface brightness.

(iii) The compact source (D) in the *Sf* component has a remarkably sharp boundary on its outer edge.

(iv) The line joining the two intense compact sources (A and D) passes very close ($< 1''$ arc) to the central source in the nucleus of the galaxy.

In addition the following deductions may be made:

(v) The density of matter in both the heads and the tails, as derived from the polarization measurements, is very small, with $N_e \lesssim 10^{-3}$ cm^{-3}.

(vi) All of the relativistic electrons responsible for the radio emission are

produced in the compact heads and diffuse into the tail on a time scale of $\sim 4 \times 10^4$ yr.

Our conclusions concerning the relevance of various source models may be summarized as follows:

Although (iii) suggests an interaction of some sort between the heads and an intergalactic gas, (v) excludes both inertial and de Young & Axford ram-pressure models. The bubble model of Gull & Northover overcomes (v), but on this model (iv) is too improbable and (iii) has no explanation. Although a source of energy might exist in each of the compact heads, as in the model of Burbidge (1967) in which massive collapsed objects are supposed to be ejected from the nucleus of the galaxy, it seems difficult to account for an adequate source of energy. It seems more probable that the origin of the relativistic electrons lies in the continuing ejection of beams of energetic particles or low frequency waves from the nucleus of the galaxy, whose radio emission indicates it to be a continuing source of energy. The interaction of these beams with the heads provides the most satisfactory explanation for the compact components, whilst the diffusion of relativistic particles into the extensive tails could account both for their total emission and their steep spectra.

ACKNOWLEDGMENTS

We thank our colleagues, especially Dr G. G. Pooley, for their assistance with the observations. We are also indebted to Drs J. E. Baldwin, M. S. Longair, P. A. G. Scheuer and J. R. Shakeshaft for valuable discussions on the interpretation of the results.

We also thank Dr B. Rowson for providing us with unpublished data on his 158 MHz observations.

One of us (P.J.H.) is indebted to the Science Research Council for a Research Studentship.

Mullard Radio Astronomy Observatory, Cavendish Laboratory, Cambridge

REFERENCES

Baade, W. & Minkowski, R., 1954. *Astrophys. J.*, **119**, 206.
Basart, J. P., Clark, B. G. & Kramer, J. S., 1968. *Publ. astr. Soc. Pacific*, **80**, 273.
Bridle, A. H., 1967. *Observatory*, **87**, 60.
Burbidge, G. R., 1967. *Nature, Lond.*, **216**, 1287.
De Young, D. S. & Axford, W. I., 1967. *Nature, Lond.*, **216**, 129.
Erickson, W. C., Kuiper, T. B. H., Clark, T. A., Knowles, S. H. & Broderick, J. J., 1972. *Astrophys. J.*, **177**, 101.
Gol'nev, V. J. & Soboleva, N. S., 1965. *Astr. Zh.*, **42**, 694 and *Sov. Astr. — AJ*, **9**, 537.
Griffin, R. F., 1963. *Astr. J.*, **68**, 421.
Gull, S. F. & Northover, K. J. E., 1973. *Nature, Lond.*, **244**, 80.
Harris, A. B., 1974. *Mon. Not. R. astr. Soc.*, **166**, 449.
Hinder, R. & Ryle, M., 1971. *Mon. Not. R. astr. Soc.*, **154**, 229.
Hollinger, J. P., Mayer, C. H. & Menella, R. A., 1964. *Astrophys. J.*, **140**, 656.
Kellermann, K. I., Pauliny-Toth, I. I. K. & Williams, P. J. S., 1969. *Astrophys. J.*, **157**, 1.
Longair, M. S., Ryle, M. & Scheuer, P. A. G., 1973. *Mon. Not. R. astr. Soc.*, **164**, 243.
Macdonald, G. H., Kenderdine, S. & Neville, A. C., 1968. *Mon. Not. R. astr. Soc.*, **138**, 259.

Mackay, C. D., 1973. *Mon. Not. R. astr. Soc.*, **162,** 1.
Miley, G. K. & Wade, C. M., 1971. *Astrophys. Letters*, **8,** 11.
Mills, D. M. & Sturrock, P. A., 1970. *Astrophys. Letters*, **5,** 105.
Mitton, S., 1971. *Mon. Not. R. astr. Soc.*, **153,** 133.
Mitton, S., 1973. *Astrophys. Letters*, **13,** 19.
Mitton, S. & Mitton, J., 1972. *Mon. Not. R. astr. Soc.*, **158,** 245.
Mitton, S. & Ryle, M., 1969. *Mon. Not. R. astr. Soc.*, **146,** 221.
Readhead, A. C. S. & Hewish, A., 1972. *Nature, Lond.*, **236,** 440.
Rees, M. J., 1971. *Nature, Lond.*, **229,** 312.
Rowson, B., 1963. *Mon. Not. R. astr. Soc.*, **125,** 177.
Ryle, M., 1972. *Nature, Lond.*, **239,** 435.
Scheuer, P. A. G., 1967. *Plasma astrophysics*, p. 262, ed. P. A. Sturrock, Academic Press, London.
Scheuer, P. A. G., 1974. *Mon. Not. R. astr. Soc.*, **166,** 513.
Schmidt, M., 1965. *Astrophys. J.*, **141,** 1.
Schraml, J. & Turlo, Z., 1967. *Astrophys. J.*, **150,** L15.
Slee, O. B. & Wraith, P. K., 1967. *Nature, Lond.*, **214,** 971.
Slysh, V. I., 1965. *Astr. Zh.*, **42,** 689, and *Sov. Astr. — AJ*, **9,** 533.